Electronic and Optical properties of Bi_2Te_3Thin Film: A First Principles Calculations Within Cooper's Exchange Potentials

Abdullahi Lawal[1*],A. B Suleiman[2], A. S Gidado[3],

[1]Department of Physics, Federal College of Education Zaria, P.M.B 1041 Zaria, Kaduna State, Nigeria
[2]Department of Physics, Federal University Dutse, Jigawa State, Nigeria
[3]Department of Physics,Bayero University Kano, PMB 3011 Kano, Nigeria

[*]abdullahikubau@yahoo.com

Abstract

Bismuth telluride (Bi_2Te_3) thin film have received great interests forlaser photonic, optical communication, biomedical imaging,gas sensingand motion detectionapplications. Therefore, to expose its hidden potentials, detailed knowledge ofits optoelectronic properties at the level of reliable and more efficienttechniques is very essential.In this study, theoretical calculations ofelectronic and optical properties of Bi_2Te_3 thin filmsare presented using first principles approachbased on recent developed Cooper's exchange potentials (vdW-DF^{C09}x) within Density Functional Theory (DFT) framework.The simulated film is in the [001] direction using supercell method with a large vacuum along z-direction so that slab and periodic images can be treated independently. The calculated values ofdirect energy gap at Γ point confirmed the robust surface states from 3quintuple layer (QL). The 1QL, 2QL, 3QL and 4QL films show an energy gap of 0.421, 0.122, 0.023 and 0.006 eV respectively and these values are in good agreement with experimental results.Optical properties comprising ofimaginary and real parts ofdielectric function, electron loses function and absorption coefficientwere also investigated to understand the optical behaviour of Bi_2Te_3 thin films.Theresults of optical absorption show that Bi_2Te_3thin film has strong absorption in the near infrared to ultraviolet wavelenghts, therefore, it is anticipated that these films can be used as an absorbing layer for broadband photodetector and solar cell.

Keywords:Bi_2Te_3, Photodetector, vdW-DF^{C09}x, DFT

INTRODUCTION

For the last few decades, achievement of useful high performance broadband photodetector in terms of quantum efficiency, speed and responsivity remain challenging for researchers. It was found from experimental and theoretical studies that second generation topological insulators (2GTIs), mainly Sb_2Te_3, Bi_2Te_3 and Bi_2Se_3 havemetallic phase along the layer surface, strong light absorption, small band gap energy in the bulk form, single Dirac cone at the surface, low saturable optical intensity, saturable absorber behaviour,high damage threshold, large modulation depth, and low cost [1-4]. However, this exotic metallic state and stong light absorptions renders these novel materials suitable for optoelectronic applications, especially broadband photodetector[5, 6].Xiaet al. demonstrated that topological nature in 2GTs is strongly depends on strong spin-orbit coupling (SOC) and is protected by time-reversal symmetry[7].Also, Yan et al. reported that presence of strong SOC in these compounds reduces the probability of the electrons in metallic surface states being backscattered by the surface defects[8]. Experimental and theoretical investigations have shown that materials with single Dirac cone along the layer surface are promising candidates for optoelectronic applications[9-11].Experimental measurements haverevealed that these materials are spin-momentum locked due to the presents of strong SOC and the spin polarization is determines with respect to the direction of their motion [12]. It is also well known that these compounds are belongs to rhombohedral structure with (R-3m) space group containing five atoms per unitcell.Alternatively three rhombohedral crystal structure form hexagonal structure similar to graphene with 15 atoms per unit cell. It is clear within hexagonal crystal structure that 2GTI TIs are layered compounds in the form of slab with five atomic layer. Each of Te-1(Se-1)-Sb (Bi)-Te-2 (Se-2)-Sb (Bi)-Te-1 (Se-1) forms what is called quintuple layer (QL) as can be seen in Fig 1. These QLs are held together along vertical direction by weak der Waals interactions andstrong bonds insides the QLknown as covalent bonding [13, 14]. Although, vdW interaction is weak but it played an important role in interactions between layers separated by empty space or atoms[15]. The space

group represents the symmetry operation for forming larger structure when performed on primitive unit cell. The “3” and “m” in the space group refer to rotation inversion and mirror.Although extensive studies have been performed for Bi_2Te_3, most of the studies focused of its potentiality of converting heat into electrical energy,its optoelectronic behaviour is scarcely studied. This research offers comprehensive study on optoelectronic properties of Bi_2Te_3surface state via first-principlesapproach within most recent developed Cooper’s exchange potential (vdW-DF^{C09}x)[16], in order to spawn a new generation high performance broadband photodetector for our daily lives benefits.Therefore, for a better understanding of its optoelectronic behavior in 2D, detailed knowledge of theelectronic and optical properties ofBi_2Se_3 surface states at the level of more efficient and reliable techniques is essential to expose its hidden potential fordevice applications such as photo-detectors.It has been established that first-principles many-body calculations would be suitable with fully self-consistent or noneself-consistent GW, because it provides true quasiparticle energies [17]. However,self-consistent and nonself-consistent GW approaches are computaionally prohibited for surface statecalculations of 2GTIs [18]. Conversely, it is generally accepted that first-principles calculation based onlocal density approximation (LDA) and generalised gradient approximation of PBE [19]are practical for surface states calculations[14, 18, 20-22].Therefore, this work describe the implementation of first-principles approach to study the electronic band structure and optical properties ofBi_2Te_3 surface states. To the best of our knowledge, surface state electronic band structure and optical properties calculation of $Bi_2Te_3$with most resent Cooper’s exchange functionals (vdW⁻DF^{C90}x)[16]have not reported yet. The surface states electronic band structures and optical properties of Bi_2Se_3 films are calculated using PBE+vdW-DFC^{09}x by varying the thickness from 1 to 4QLs.

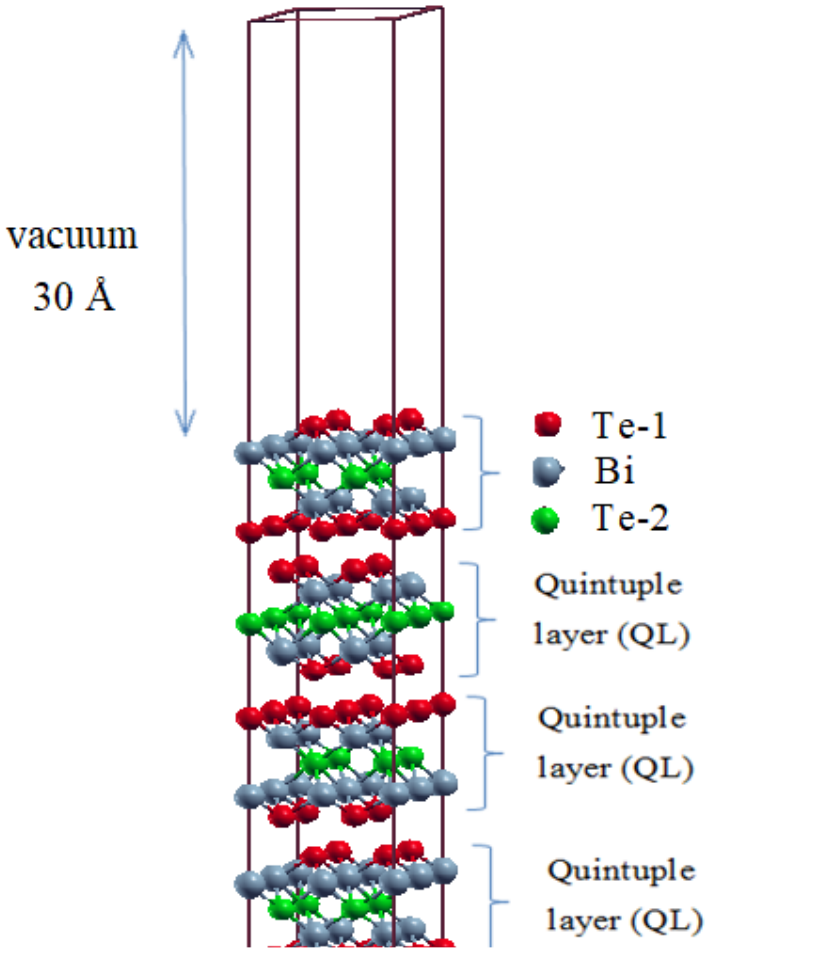

Fig 1:(a) Crystallographic geometry of Bi_2Te_3thin film

Conversion of DFT into Practical Tool

THEORETICAL METHODOLOGY

DTF is a quantum mechanical theory widely used in physics and chemistry. Over the past decades, much attention has been focused on using DFT-based approaches to materials properties.Density functional theory (DFT) is a universal approach to the quantum mechanical many-body problem, where the system of interacting electrons is mapped in a unique manner onto

an effective non-interacting system with the same total density [23]. DFT is used to calculate the properties of simple to complex systems that contain many atoms such as large molecules or solids. In DFT, the calculations were simplified by applying the periodic boundary conditions, translational and point group symmetry operations. As well known, DFT is an established and powerful approach for the solution of many-body problem of Schrodinger equation. In 1998, Hohenberg and Kohn [24] have received a noble prize in chemistry by proposing DFT to simplify the calculations of electronic properties in solids. It became a study theory after the introduction of two theorems by Hohenberg and Kohn. Calculations based on DFT are distinguished from other *ab initio* approaches as first-principles calculation with an approximate error of 10^{-3} eV, the errors can be minimized by adjusting the cut-off energy or k-points mesh. In many cases, the first-principles approach within the framework of DFT gives accurate predictions of various properties of materials, stable configuration and total energy. Interestingly, the computational costs of DFT is comparatively low [3].

The calculations presented in this work are performed within two open source simulation packages Quantum Espresso [25] and YAMBO [26] codes and all calculationsare performed at room-temperature.Full relativistic norm-conserving pseudopotentials generated using Rappe-Rabe-Kaxiras-Joannopoulos (RRKJ) technique were used to model the interactions between the valence electronand ionic core potential of Bi, Te-1, and Te-2atoms withinclusion of spin-orbit coupling (SOC). An electron orbital of $6s^2$ $6p^3$ $5d^{10}$ and $5s^2$ $5p^4$for Bi and Tewere used as valence electrons throughout the calculations. The surface state band structure calculations of B_2Te_3 have been performed within 1 to 4 quintuples (QLs) slabs. To avoid unwanted interactions between the nearest slabs, a large vacuum layer of 30 □ was used so that periodic images and the layer can be treated independently as can be seen in Fig. 1. A 12×12×1 k-point mesh grid was used for the integration of the Brillouin zone (BZ). Plane-wave basis set with kinetic energy cut-offs of 80 Ry was used to expand the electron wave functions and 450 Ry for charge density. Also, the atomic positions, the

size and the shape of the supercell slab geometry are relaxed until Hellmann-Feynman forces acting on each ion becomeless than10^{-3} eV/Å.

RESULTS AND DISCUSSION

3.1 Electronic Properties

This section describes the implementation of first-principles approach to study the surface states ofBi_2Te_3. However, due to the limitation of computational resources, thin film calculations with more than 4 quintuple layers (QLs) are not performed in this work, because as slab thickness increases the time cost for the first-principles calculations also increases very rapidly. The calculated band dispersions of Bi_2Te_3 slabs within PBE+vdW-DF^{C09}x functional with thickness from 1QL to 4QL along special symmetry directions of the irreducible Brillouin zone setting Fermi energy level scale at 0 eV are presented in Fig 2.The selected high symmetry points are $K\left(\frac{1}{3},\frac{2}{3},0\right)$, $\Gamma(0,0,0)$ and $M\left(0,\frac{1}{2},0\right)$ respectively.The calculated band structure results of Bi_2Te_3 with the bottom and top faces terminated by Te-2 show that when the film thickness is less than 4QL an energy gap at Γ point is formed. These gaps are due to hybridization between the wavefunctions of the surface states at the top and the bottom of the thin slabs. For 1QL film the interactions between the bottom and the top surfaces is very strong to open up a very large energy gap at Γ point. The interaction between the bottom and the top surfaces becomes progressively weaker from 2QL film. The nature of the topological feature start to exist from the 2QL film as can be seen in Fig2. Also, the linear even combination at Γ point of the bottom spin-up and the top spin-up surface states are degenerate with respect to the linear even combination of the bottom spin-down and the top spin-down surface states. On the other hand, the magnitudes of the gap reduce drastically with increasing film thickness.At 4QL the energy gap at Γ point is almost zero because the interaction between the top surface bands and bottom surface bands is minimal. The “M” shape of the valence band (VB) at

the bottom in the electronic band structure of Bi_2Te_3 films and the magnitude of both indirect gap and the energy gap at Γ point are in good agreement with experimental measurement [27].

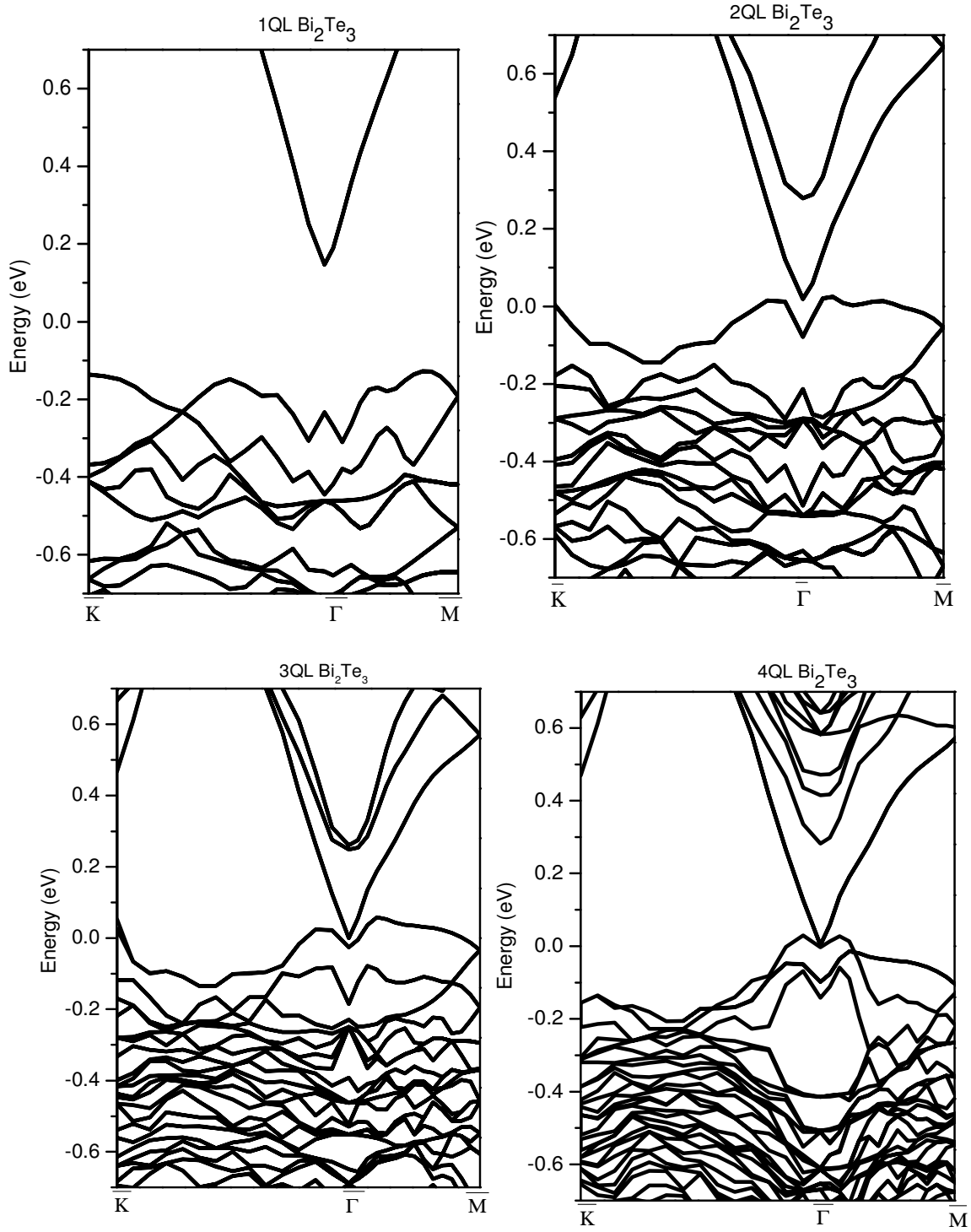

Fig.2**:** Band structures of Bi_2Te_3 films with 1QL, 2QL, 3QL and 4QL

Table 1: Calculated indirect $\mathbf{E_{ind}}$ and direct $\mathbf{E_{\Gamma}}$ energy gaps at **Γ** point results for Bi_2Te3 film in function of slab thickness

	1 QL	2 QL	3 QL	4 QL
E_{Γ} (eV)	0.421	0.122	0.023	0.006
E_{ind} (eV)	0.11	No gap	No gap	No gap

Besides the "M" shape of the VB at the bottom, the massless Dirac-like surface states can also be clearly seen in Fig2 as linear band dispersion. This feature is in quite agreement with recent angle-resolved photoemission spectroscopy measurements [28, 29] and theoretical predictions [30-32]. The calculated values of direct energy gap at Γ point confirmed the robust surface states from 3QL. The 1QL, 2QL, 3QL and 4QL films show energy gap of 0.421, 0.122, 0.023 and 0.006 eV respectively. These values are in quite good agreement with experimental results 0.11 eV for 2 QL [33], 0.03 for 3QL [27].

3.2 Optical properties

The study of optical properties of a material is crucial to get insight view about its characteristics forapplication in the optoelectronic system and devices.From the literature review, it was found that the exploration of the optical features of Bi_2Te_3 thin filmsarescarcely done. To complete the study on the optoelectronic propertiesin addition to the electronic properties, a comprehensive study is presented on the optical properties ofBi_2Te_3 thin filmby most recentCoope's exchange functional (vdW-DF^{C09}x)[16]. The optical parameters investigated in this research work are real $\varepsilon_1(\omega)$ and imaginary$\varepsilon_2(\omega)$ parts of frequency-dependent dielectric function, absorption coefficient, $\alpha(\omega)$ and electron energy loss spectrum (EELS). Hence, by adopting Quantum

Espresso[25] and YAMBO[26]packages, these properties have been obtained and discussed in detail.Optical parameters of material normally explain the behavior of the material when exposed to the electromagnetic radiation and they also help in predicting band structure configuration. Therefore, understanding optical behavior of a material is essential to evaluation its usefulness and applicability for optoelectronic application [34]. It has been established that optical behavior is strongly associated with electronic structure[35]. As observed in the electronic band structure analysis, the geometry of the electronic structure for Bi_2Te_3 thin films changed with films thickness. Several experimental studies have showed that optical properties of Bi_2Te_3 thin film dependent on the thickness of the film[36-38]. Due to the limitation of computational resources, optical properties calculations are performed on 3 QLs, because as slab thickness increases the time cost for the first-principles calculations increases very rapidly.However, to the best of our knowledge theoretical investigation on Bi_2Te_3 thin filmhave not been reported yet on optical properties. In order to describe the said parameters quantitively, it is essential to evaluate the dielectric function. Dielectric function is the ratio of the permittivity of a material to the permittivity of free space, and permittivity is the measure of the resistance of a material when an electric field is induced in a material. Alldielectric materials are insulators but allinsulators are not dielectric [39]. The dielectric function consists of real ($\varepsilon_1(\omega)$) and imaginary part ($\varepsilon_2(\omega)$). It is represented as follows:

$$\varepsilon(\omega) = \varepsilon_1(\omega) + i\varepsilon_2(\omega) \quad (1)$$

where $\varepsilon_1(\omega)$ is real part and $\varepsilon_2(\omega)$ is imaginary part of the dielectric function. Physical properties and band structure rely strongly on $\varepsilon(\omega)$. As mentioned, we analyzed the optical properties based on Coope's exchange functional (vdW-DF^{C09}x).From the knowledge of electronic band structure of a solid, the imaginary part ofdielectric function, $\varepsilon_2(\omega)$ can be calculated from Kubo–Greenwood equation as show in Equation 2:

$$\varepsilon_2(\omega) = \frac{2\pi e^2}{\Omega \varepsilon_0} |\langle \psi_k^c | \hat{u} \times \vec{r} | \psi_k^v \rangle| \delta\left(E_k^c - (E_k^v + E)\right) \quad (2)$$

Once we know the imaginary part, the real part, $\varepsilon_1(\omega)$ can be obtain from the Kramers–Kronig relations in Equation 3[40].

$$\varepsilon_1(\omega) = 1 + \left(\frac{2}{\pi}\right) \int_0^\infty d\omega' \frac{\omega'^2 \varepsilon_2(\omega')}{\omega'^2 - \omega^2} \quad (3)$$

$$\alpha(\omega) = \frac{\omega}{c} \sqrt{2 \left(\sqrt{\varepsilon_1^2(\omega) + \varepsilon_2^2(\omega)} - \varepsilon_1(\omega) \right)} \quad (4)$$

$$n(\omega) = \sqrt{\left(\frac{\sqrt{\varepsilon_1^2(\omega) + \varepsilon_2^2(\omega)} + \varepsilon_1(\omega)}{2} \right)} \quad (5)$$

$$k(\omega) = \sqrt{\frac{\sqrt{\varepsilon_1^2(\omega) + \varepsilon_2^2(\omega)} - \varepsilon_1(\omega)}{2}} \quad (6)$$

$$L(\omega) = \frac{\varepsilon_2(\omega)}{\varepsilon_2(\omega) + \varepsilon_1(\omega)} \quad (7)$$

The real part of a macroscopic dielectric function describes how much material has been polarized as a result of induced electric dipole creation by an external field, and the imaginary part describes how much material capacity is for the absorption of photon energy. The electronic contributions at high frequency and ionic contributions of a non-polar system are contained in the static dielectric permittivity tensor $\varepsilon(0)$. The calculated imaginary (ε_2) and the real (ε_1) parts of dielectric functions as a function of photon energy are shown in Fig 3(a)-(b). The static dielectric constant, $\varepsilon_1(0)$ is the value of real partof dielectric constant at zero energy. This parameter was analyzed for Bi_2Te_3 thin film as can be seen in Fig 3(a). From the results, it is noticed that the value of static dielectric constant was found to be 33.6. Conversely, this value isan important parameter that can be used to obtain the energy band gap valueof Bi_2Te_3 thin filmvia Penn Model relation $\varepsilon_1(0) \approx \left(\hbar\omega_p / E_g\right)^2 + 1$[41]. By using plasma energy $\hbar\omega_p$ and the value of $\varepsilon_1(0)$, the value of the energy band gap of the title material can be calculated. Thus, the change in the real part of dielectric

function from positive to negative at about 2.8 eV, indicates that the material under investigation should resonate at energy greater than 2.8 eV.The epsilon-near-zero behavior of Bi_2Te_3 is another exciting feature for its versatile applications [42-44]. It has been established that imaginary part of the dielectric function is directly connected with the energy band structure. The edge of optical absorption (first critical point) occurs at about 0.023 eV, this value is related to band gap value. Hence, the calculated imaginary part of dielectric function shows that the first critical point is related to the transition from valence band maximum to the conduction band minimum which correspond to the fundamental band gap. The results of imaginary part of dielectric function indicated that Bi_2Te_3 thin film has good absorption behavior in the near infrared to visible light wavelengths, which depicts its suitability for laser photonic, optical communication, biomedical imaging, remote sensing, solar cell and gas sensing applications.Absorption coefficient gives information on the extent with which a material absorbs photon energy. When light rays strike the surface of a material, part of its energy is transferred to the surface while some arereflected back. This transfer of energy to the surface is called absorption of light. It is represented in terms of absorption coefficient $\alpha(\omega)$.

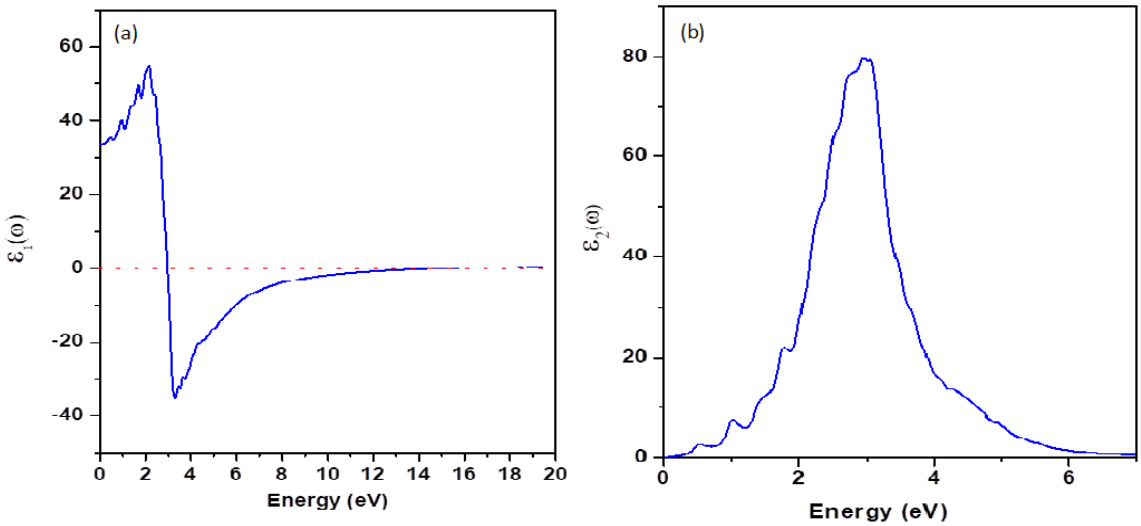

Fig. 3 (a) Energy spectra real part of dielectric function (b) Energy spectra imaginary part of dielectric functionalong (1 0 0) axis.

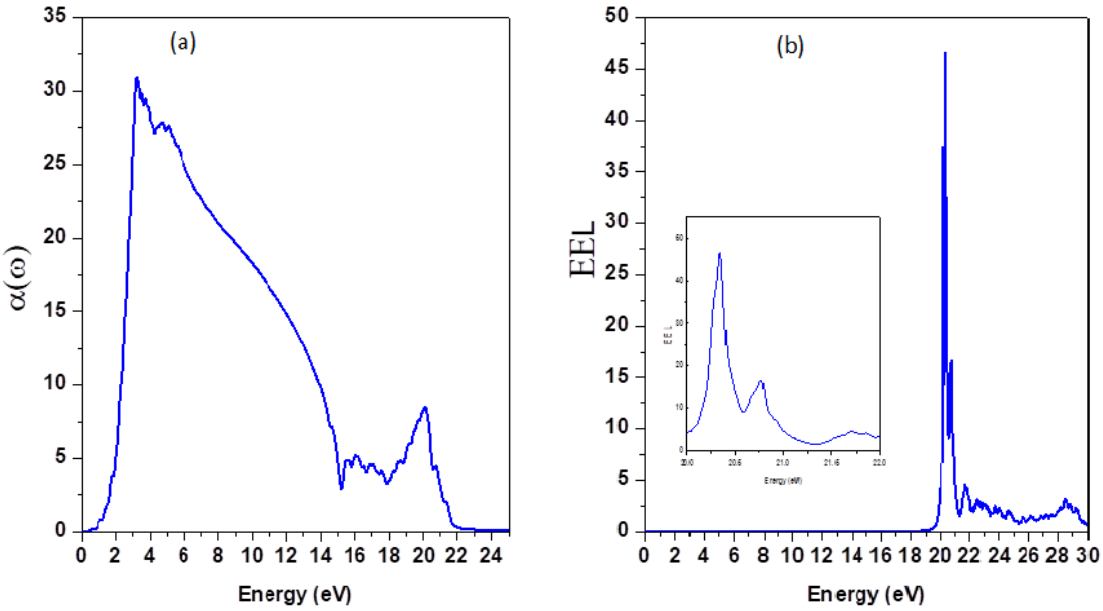

Fig. 4(a) Energy spectra of absorption coefficient $\alpha(\omega)$(b)EELs of Bi_2Se_3 surface states calculated using vdW-DF^{C09}x.

Graph of absorption coefficient as a function of the photon energy is presented in Fig. 4(a).The variation of optical absorption with photon energy indicates the prospective use of Bi_2Te_3 thin films for device applications, which can be operated over a wider range of energy scale.Electron energy loss functions is a tool that describes the loss in energy of a fast moving electron in a material from the top of a valence band to bottom of a conduction band[45]. In this energy distribution, impinging electrons can be categorised in three ways. First category of electrons loses a part of their energy by exciting electrons in the outer shells which resulted in valence inter-band transitions. The second category of electrons is responsible for excitations in the inner shell electrons. The third category of electrons either remains un-scattered or interreact elastically. The graph of energy loss function is represented in Fig. 4 (b). EELs were obtained over a wide range of energy (0-30 eV) and the highest value of its prominent loss region represents $\hbar\omega_p$. The feature behaviour of the prominent peaks in the spectra represents the characteristics of plasma resonance which was found to be 20.3 eV. This sharp maximum peak of the energy loss function spectra appears at a particular incident light frequency which corresponds to the trailing edges in the

reflection spectra sometimes called plasma frequency ω_P. At this point of energy, the real part of the dielectric function goes to zero indicating rapid reduction in reflectance. The sharp maxima peak of the energy loss function spectra is related to an abrupt reduction in reflection spectra.

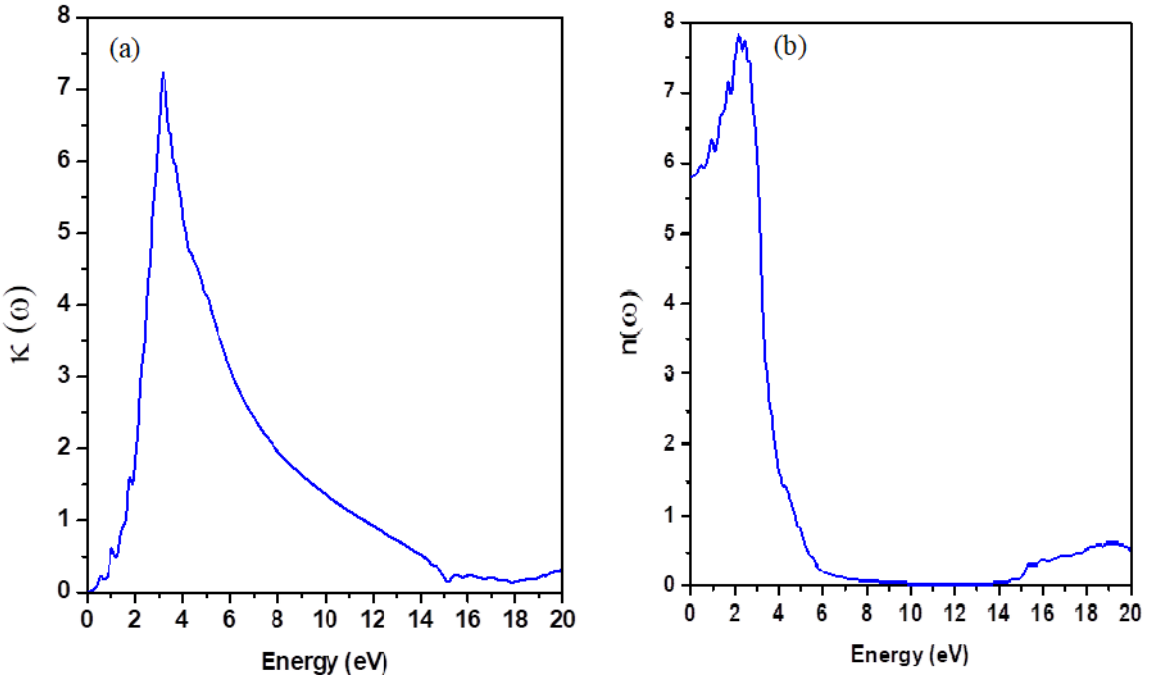

Fig. 5(a) Energy spectra of absorption coefficient $\alpha(\omega)$ (b)EELs of Bi_2Se_3 surface states calculated using vdW-DF^{C09}x.

The refractive index **n** of the material is defined as the ratio of the velocity of light in a vacuum (c) to the light velocity in medium (υ) [30].

Mathematically,

$$n = \frac{c}{\upsilon}$$

Where refractive index depends on the wavelength of light. Greater the wavelength of light, lesser is the index of refraction and lesser the wavelength, greater is n. The velocity c is related to the electric and magnetic permeability of vacuum i.e. $\epsilon_0$and $\mu_0$respectively. The refractive index is a quantity that describes how much light is refracted after entering material [46]. Fig. 5(a) and (b)

show the refractive index $n(\omega)$and extinction index $k(\omega)$of Bi_2Te_3thin film as a function of energy.The static refractive index was found to be 5.7 and this value is in good agreement with experimental measurement [47].From the refractive index graph, we note that the material possesses high refractive index within visible lightregion around 2.3 eV and decreases at higher energy in the visible to UV region. Furthermore, above 4.2 eV the velocity of light is greater than the light celerity because $n(\omega)$ is less than one. Also, refractive index graph indicates that the material generated high output at low energy because the highest index value is between 0-3 eV. In the energy range from 0 to 0.023 eVthe calculated $k(\omega)$ is less than 0.1 indicating that Bi_2Te_3thin film material response to light with wavelength below 54 μm and then increases rapidly with photon energy forming the maximum peak at 3.2 eV.

CONCLUSIONS

In summary, the electronic and optical propertiesof Bi_2Te_3 thin films has been performed using first-principles calculations based on density functional theory (DFT) framework within the most recent developed Coope's exchange (vdW-DF^{C09}x). The band dispersions calculations of Bi_2Te_3 films show that this material possess robust surface states. The band dispersions calculations of Bi_2Se_3films with van der Waals interaction reveal that; at the thinner film, the strong interaction between the bottom surface and top surface bands resulted in an energy gap at Γ point and the magnitude of the gap decays rapidly by increasing the thickness of the film. The 1QL, 2QL, 3QL and 4QL films show an energy gap of 0.421, 0.122, 0.023 and 0.006 eV respectively. On the other hand, the values of the band gap at Γ point are in quite agreement with the available experimental measurements when compared with bare PBE and GW results. Moreover, it has been found that Kohn-Sham DFT with inclusion of SOC and vdW interactions is able to provide correct description of the topologically nontrivial electronic band structures of Bi_2Se_3. Interestingly, the Dirac point is located well inside the band gap.The Results of optical absorption shows that Bi_2Te_3 thin film has strong absorption in the near infrared to ultraviolet wavelenghts, therefore, it can be used in optoelectronics devices such as laser photonic, optical communication, biomedical imaging, remote sensing, solar cell and gas sensing.

REFERENCES

1. Lee, J.; Koo, J.; Chi, C.; Lee, J. H. In *A harmonically mode-locked femtosecond fiber laser using bulk-structured Bi 2 Te 3 topological insulator*, 2015 Conference on Lasers and Electro-Optics (CLEO), 2015; IEEE: pp 1-2.
2. Hasan, M. Z.; Kane, C. L., Colloquium: topological insulators. *Reviews of Modern Physics* **2010,** 82, (4), 3045.
3. Lawal, A.; Shaari, A.; Ahmed, R.; Jarkoni, N., First-principles investigations of electron-hole inclusion effects on optoelectronic properties of Bi2Te3, a topological insulator for broadband photodetector. *Physica B: Condensed Matter* **2017,** 520, 69-75.
4. Das, B.; Das, N. S.; Sarkar, S.; Chatterjee, B. K.; Chattopadhyay, K. K., Topological Insulator Bi2Se3/Si-Nanowire-Based p–n Junction Diode for High-Performance Near-Infrared Photodetector. *ACS applied materials & interfaces* **2017,** 9, (27), 22788-22798.
5. Lawal, A.; Shaari, A.; Ahmed, R.; Taura, L.; Madugu, L.; Idris, M., Sb2Te3/graphene heterostructure for broadband photodetector: A first-principles calculation at the level of Cooper's exchange functionals. *Optik* **2019,** 177, 83-92.
6. Yang, M.; Wang, J.; Zhao, Y.; He, L.; Ji, C.; Liu, X.; Zhou, H.; Wu, Z.; Wang, X.; Jiang, Y., Three-Dimensional Topological Insulator Bi2Te3/Organic Thin Film Heterojunction Photodetector with Fast and Wideband Response from 450 to 3500 Nanometer. *ACS nano* **2018**.
7. Xia, Y.; Qian, D.; Hsieh, D.; Wray, L.; Pal, A.; Lin, H.; Bansil, A.; Grauer, D.; Hor, Y. S.; Cava, R. J., Observation of a large-gap topological-insulator class with a single Dirac cone on the surface. *Nature physics* **2009,** 5, (6), 398.
8. Yan, B.; Stadtmüller, B.; Haag, N.; Jakobs, S.; Seidel, J.; Jungkenn, D.; Mathias, S.; Cinchetti, M.; Aeschlimann, M.; Felser, C., Topological states on the gold surface. *Nature communications* **2015,** 6, 10167.
9. Kim, J.; Jang, H.; Koirala, N.; Sim, S.; Lee, J.-b.; Kim, U. J.; Lee, H.; Cha, S.; In, C.; Park, J. In *Gate-tunable, high-responsivity, and room-temperature infrared photodetectors based on a graphene-Bi 2 Se 3 heterostructure*, Lasers and Electro-Optics (CLEO), 2016 Conference on, 2016; IEEE: pp 1-2.
10. Yao, J.; Shao, J.; Wang, Y.; Zhao, Z.; Yang, G., Ultra-broadband and high response of the Bi 2 Te 3–Si heterojunction and its application as a photodetector at room temperature in harsh working environments. *Nanoscale* **2015,** 7, (29), 12535-12541.
11. Xu, J.; Zhao, Y.; Wen, K.; Tu, J., Ultracompact optical hybrid based on standing wave integrated with graphene-based photodetector for coherent detection. *IEEE Photonics Journal* **2018**.
12. He, Q. L.; Lai, Y. H.; Lu, Y.; Law, K. T.; Sou, I. K., Surface reactivity enhancement on a Pd/Bi 2 Te 3 heterostructure through robust topological surface states. *Scientific reports* **2013,** 3, 2497.
13. Aguilera, I.; Friedrich, C.; Bihlmayer, G.; Blügel, S., G W study of topological insulators Bi 2 Se 3, Bi 2 Te 3, and Sb 2 Te 3: Beyond the perturbative one-shot approach. *Physical Review B* **2013,** 88, (4), 045206.
14. Zhang, Y., Communication: Surface stability and topological surface states of cleaved Bi2Se3: First-principles studies. AIP Publishing: 2015.
15. Ambrosetti, A.; Silvestrelli, P. L., Hidden by graphene--towards effective screening of interface van der Waals interactions via monolayer coating. *arXiv preprint arXiv:1806.04394* **2018**.
16. Cooper, V. R., Van der Waals density functional: An appropriate exchange functional. *Physical Review B* **2010,** 81, (16), 161104.
17. Hybertsen, M. S.; Louie, S. G., Electron correlation in semiconductors and insulators: Band gaps and quasiparticle energies. *Physical Review B* **1986,** 34, (8), 5390.
18. Crowley, J. M.; Tahir-Kheli, J.; Goddard III, W. A., Accurate Ab Initio Quantum Mechanics Simulations of Bi2Se3 and Bi2Te3 Topological Insulator Surfaces. *The journal of physical chemistry letters* **2015,** 6, (19), 3792-3796.
19. Perdew, J. P.; Burke, K.; Ernzerhof, M., Generalized gradient approximation made simple. *Physical review letters* **1996,** 77, (18), 3865.
20. Popov, I.; Mantega, M.; Narayan, A.; Sanvito, S., Proximity-induced topological state in graphene. *Physical Review B* **2014,** 90, (3), 035418.

21. McIver, J.; Hsieh, D.; Drapcho, S.; Torchinsky, D.; Gardner, D.; Lee, Y.; Gedik, N., Theoretical and experimental study of second harmonic generation from the surface of the topological insulator Bi 2 Se 3. *Physical Review B* **2012,** 86, (3), 035327.
22. Zhang, H.; Liu, C.-X.; Qi, X.-L.; Dai, X.; Fang, Z.; Zhang, S.-C., Topological insulators in Bi 2 Se 3, Bi 2 Te 3 and Sb 2 Te 3 with a single Dirac cone on the surface. *Nature physics* **2009,** 5, (6), 438.
23. Parr, R. G., *Density functional theory of atoms and molecules*. Springer: 1980.
24. Hohenberg, P.; Kohn, W., Inhomogeneous electron gas. *Physical review* **1964,** 136, (3B), B864.
25. Giannozzi, P.; Baroni, S.; Bonini, N.; Calandra, M.; Car, R.; Cavazzoni, C.; Ceresoli, D.; Chiarotti, G. L.; Cococcioni, M.; Dabo, I., QUANTUM ESPRESSO: a modular and open-source software project for quantum simulations of materials. *Journal of physics: Condensed matter* **2009,** 21, (39), 395502.
26. Marini, A.; Hogan, C.; Grüning, M.; Varsano, D., Yambo: an ab initio tool for excited state calculations. *Computer Physics Communications* **2009,** 180, (8), 1392-1403.
27. Li, Y.-Y.; Wang, G.; Zhu, X.-G.; Liu, M.-H.; Ye, C.; Chen, X.; Wang, Y.-Y.; He, K.; Wang, L.-L.; Ma, X.-C., Growth dynamics and thickness-dependent electronic structure of topological insulator Bi2Te3 thin films on Si. *arXiv preprint arXiv:0912.5054* **2009**.
28. Chen, Y.; Analytis, J.; Chu, J.-H.; Liu, Z.; Mo, S.-K.; Qi, X.-L.; Zhang, H.; Lu, D.; Dai, X.; Fang, Z., Experimental realization of a three-dimensional topological insulator, Bi2Te3. *Science* **2009,** 325, (5937), 178-181.
29. Zhang, H.; Liu, C.-X.; Qi, X.-L.; Dai, X.; Fang, Z.; Zhang, S.-C., Topological insulators in Bi2Se3, Bi2Te3 and Sb2Te3 with a single Dirac cone on the surface. *Nature physics* **2009,** 5, (6), 438-442.
30. Kato, T.; Kotaka, H.; Ishii, F., First-principles study of surface states in topological insulators Bi2Te3 and Bi2Se3: film thickness dependence. *Molecular Simulation* **2015,** 41, (10-12), 892-895.
31. Barker, B.; Deslippe, J.; Yazyev, O.; Louie, S. G. In *Quasiparticle electronic structure of bulk and slab Bi2Se3 and Bi2Te3*, APS Meeting Abstracts, 2014; p 42014.
32. Yazyev, O. V.; Moore, J. E.; Louie, S. G., Spin polarization and transport of surface states in the topological insulators Bi 2 Se 3 and Bi 2 Te 3 from first principles. *Physical review letters* **2010,** 105, (26), 266806.
33. Chen, Y.; Analytis, J. G.; Chu, J.-H.; Liu, Z.; Mo, S.-K.; Qi, X.-L.; Zhang, H.; Lu, D.; Dai, X.; Fang, Z., Experimental realization of a three-dimensional topological insulator, Bi2Te3. *science* **2009,** 325, (5937), 178-181.
34. Singh, J., *Optical properties of condensed matter and applications*. John Wiley & Sons: 2006; Vol. 6.
35. Cohen, M. L.; Chelikowsky, J. R., *Electronic structure and optical properties of semiconductors*. Springer Science & Business Media: 2012; Vol. 75.
36. He, X.; Wei, R.; Tian, X.; Qiu, J.; Zhang, M.; Zeng, Q.; Liu, J., Thermal evaporated Te-Bi2Te3 alloy thin film and its nonlinear optical properties. *Journal of Alloys and Compounds* **2017,** 714, 363-369.
37. Adam, A., Characterization of thin Bi2Te3-based films and effects of heat treatment on their optical properties. *Journal of Alloys and Compounds* **2018,** 765, 1072-1081.
38. Bahabri, F., Investigation of the structural and optical properties of bismuth telluride (Bi2Te3) thin films. *Life Sci. J* **2012,** 9, (1), 290-294.
39. Subramanian, M.; Li, D.; Duan, N.; Reisner, B.; Sleight, A., High dielectric constant in ACu3Ti4O12 and ACu3Ti3FeO12 phases. *Journal of Solid State Chemistry* **2000,** 151, (2), 323-325.
40. O'Donnell, M.; Jaynes, E.; Miller, J., Kramers–Kronig relationship between ultrasonic attenuation and phase velocity. *The Journal of the Acoustical Society of America* **1981,** 69, (3), 696-701.
41. Penn, D. R., Wave-number-dependent dielectric function of semiconductors. *Physical Review* **1962,** 128, (5), 2093.
42. Savoia, S.; Castaldi, G.; Galdi, V.; Alù, A.; Engheta, N., PT-symmetry-induced wave confinement and guiding in ε-near-zero metamaterials. *Physical Review B* **2015,** 91, (11), 115114.
43. Li, Y.; Engheta, N., Supercoupling of surface waves with ε-near-zero metastructures. *Physical Review B* **2014,** 90, (20), 201107.
44. Rodríguez-Fortuño, F. J.; Vakil, A.; Engheta, N., Electric levitation using ϵ-near-zero metamaterials. *Physical review letters* **2014,** 112, (3), 033902.

45. Kittel, C.; McEuen, P.; McEuen, P., *Introduction to solid state physics*. Wiley New York: 1996; Vol. 8.
46. Yan, W.-J.; Xie, Q.; Qin, X.-M.; Zhang, C.-H.; Zhang, Z.-Z.; Zhou, S.-Y., First-principle analysis of photoelectric properties of silicon-carbon materials with graphene-like honeycomb structure. *Computational Materials Science* **2017,** 126, 336-343.
47. Takashiri, M.; Asai, Y.; Yamauchi, K., Structural, optical, and transport properties of nanocrystalline bismuth telluride thin films treated with homogeneous electron beam irradiation and thermal annealing. *Nanotechnology* **2016,** 27, (33), 335703.